

Environment-aware communication channel quality prediction for underwater acoustic transmissions: A machine learning method [☆]



Yougan Chen ^{a,b,c,*}, Weijian Yu ^{a,b,c}, Xiang Sun ^d, Lei Wan ^{a,e}, Yi Tao ^{a,b,c}, Xiaomei Xu ^{a,b,c}

^a Key Laboratory of Underwater Acoustic Communication and Marine Information Technology (Xiamen University), Ministry of Education, Xiamen, Fujian 361005, China

^b Dongshan Swire Marine Station, College of Ocean and Earth Sciences, Xiamen University, Xiamen, Fujian 361102, China

^c Shenzhen Research Institute of Xiamen University, Shenzhen, Guangdong 518000, China

^d Department of Electrical & Computer Engineering, University of New Mexico, Albuquerque, NM 87131, USA

^e School of Informatics, Xiamen University, Xiamen, Fujian 361005, China

ARTICLE INFO

Article history:

Received 14 February 2021

Received in revised form 18 February 2021

Accepted 19 April 2021

Available online 13 May 2021

Keywords:

Underwater acoustic communications

Channel quality prediction

Energy consumption

Machine learning

ABSTRACT

Due to the limited energy supply of sensor nodes in underwater acoustic communication networks (UACNs), energy optimization for underwater acoustic transmissions is critical to prolong the network lifetime and improve network performance. Machine learning is a powerful and promising method that can be used to optimize energy consumption of UACNs. In this paper, we propose a machine learning based environment-aware communication channel quality prediction (ML-ECQP) method for UACNs. In ML-ECQP, the logistic regression (LR) algorithm is used to predict the communication channel quality (which is measured according to the bit error rate) between a transmitter and a receiver based on the perceived underwater acoustic channel environmental parameters (such as signal-to-noise ratio, underwater temperature, wind speed, etc.). Based on the predicted communication quality, each transmitter can optimize the acoustic data transmissions in order to minimize the energy waste caused by retransmissions, thus significantly reducing the energy consumption of UACNs. Extensive experiments are conducted in the Furong Lake at Xiamen University to demonstrate the performance (in terms of the feasibility, channel condition prediction accuracy, and energy consumption reduction) of the proposed ML-ECQP method.

© 2021 Elsevier Ltd. All rights reserved.

1. Introduction

Internet of underwater things (IoUT) refers to as the network of smart interconnected underwater objects to monitor vast unexplored water areas. IoUT is an enabler to achieve smart oceans, which has received growing attention from both industry and academia. In IoUT based underwater acoustic communication networks (UACNs), most of underwater acoustic devices need to be

placed underwater for a long time. However, the energy supply of these devices is usually very limited; meanwhile, it is impossible or extremely expensive (in terms of consuming tremendous manpower and material resources) to replace or recharge these devices once they are out of power [1,2]. In addition, due to the complex and dynamic features of underwater environment, the underwater acoustic channels may suffer from much stronger fading and noise interference [3,4], thus leading to retransmissions caused by packet delivery failures over the severe underwater acoustic channels. Retransmissions may significantly increase the energy consumption of underwater devices [5–7]. Therefore, it is critical to optimize the acoustic data transmissions, i.e., avoiding data transmissions when the underwater channel is bad, thus reducing the number of retransmissions and prolonging the lifetime of UACNs.

Recently, artificial intelligence (AI) technologies, such as machine learning algorithms and big data networking and analysis, have been developed and used in the fields of atmospheric science, medical, climate change, terrestrial communication, etc. [8]. Applying these AI technologies to the underwater acoustic

[☆] This work was supported in part by the Basic Research Program of Science and Technology of Shenzhen, China under Grant No. J20190809161805508, the National Key Research and Development Program of China under Grant No. 2016YFC1400200, the National Natural Science Foundation of China under Grants Nos. 41476026, 41976178, and 61801139, and the Fundamental Research Funds for the Central Universities of China under Grant No. 20720200092. Shenzhen Research Institute of Xiamen University and Key Laboratory of Underwater Acoustic Communication and Marine Information Technology (Xiamen University), Ministry of Education contributed equally to this work.

* Corresponding author at: Key Laboratory of Underwater Acoustic Communication and Marine Information Technology (Xiamen University), Ministry of Education, Xiamen, Fujian 361005, China.

E-mail address: chenyougan@xmu.edu.cn (Y. Chen).

communications is a promising way to achieve the communications much more efficient and energy-preserving.

Some researchers have explored to use of machine learning technologies to facilitate underwater acoustic communications. In the context of machine learning assisted underwater acoustic signal processing, McQuay et al. [9] proposed to use the convolutional neural network to identify the sound signal of the whale among different received signals. Roberts et al. [10] identified different fish individuals by classifying their acoustic transmissions based on the support vector machine (SVM) algorithm. In [11], in order to distinguish different underwater targets, Chen et al. adopted the deep learning algorithm to recognize different types of noise radiated by different targets. Based on the sample selection and feature selection, Yang et al. [12] proposed an underwater acoustic target recognition method by using the adaptive boosting algorithm to integrate several weak classifiers. In the context of machine learning assisted underwater acoustic localization, Pinheiro et al. [13,14] combined the SVM algorithm with the nuclear regression method to eliminate the outliers in received acoustic signals and improve the positioning accuracy of autonomous underwater vehicle (AUV). In [15], Ludwig et al. combined the deep neural network and the range estimation to realize the underwater localization for single sensor, small array, and small aperture towing array, respectively. In the context of machine learning assisted routing design in UACNs, the reinforcement learning technology is adopted to optimize the routing paths for the underwater acoustic sensor networks in order to achieve energy saving and efficient transmissions [16,17]. In [18–20], the ant colony optimization algorithm is used to design routing paths for different proposed network models to achieve different objectives, such as increasing network throughput and reducing the overall transmission distance. In [21], the authors argued that applying a machine learning algorithm to determine the routing path may perform differently under different scales of networks. They proposed the ant colony optimization algorithm-artificial fish swarm algorithm (ACOAFSA) fusion dynamic coded cooperation routing method to adaptively adopt different machine learning algorithms under different scales of UACNs. All the mentioned works apply various machine learning methods to facilitate underwater acoustic communications. Yet, none of them apply machine learning algorithms to estimate the quality of underwater acoustic channels. Note that the quality of the underwater acoustic channel is determined by many factors (such as wind speed, water surface temperature, etc.), and thus it is impossible to derive an empirical model to estimate the channel quality. The motivation of the paper is to use the logistic regression (LR) algorithm to estimate the underwater acoustic channel quality, and the estimated channel quality is used to optimize the data transmissions scheduling to reduce the energy consumption of a transmitter in UACNs.

The LR algorithm is a typical classification algorithm. LR learns/trains the mapping from input features to output labeled results based on the labeled data, and applies the well-trained mapping to the unknown data in order to achieve classification. As a typical classification algorithm, the LR algorithm has been widely used in different applications. For example, Ayalew et al. [22] used the LR algorithm to investigate the landslide susceptibility of mountains. Cannarile et al. [23] used the LR algorithm to diagnose faults of on-board aeronautical systems. Yu et al. [24] applied the LR algorithm to the load allocation improvement for a chiller system in an institutional building. Yang et al. [25] used the LR algorithm to analyze the risk of malaria in African children. Seo et al. [26] proposed the LR based target recognition model, which can improve recognition accuracy under a shallow water environment. Kalaiarasu et al. [27] applied the LR algorithm to capture the spatio-temporal variation in the performance of a UACN. The reason of the LR algorithm being widely used is because its low complexity, efficient, easy to

achieve parallel processing, and capable of realizing online learning. In addition, the LR model has strong explanatory ability, i.e., it is easy to understand the principle/reason of the classification decision made by the model.

In this paper, in order to solve the problem of energy optimization in UACNs, we propose machine learning based environment-aware communication channel quality prediction (ML-ECQP) method, where the LR algorithm is adopted to predict underwater acoustic communication quality. The main contributions of this paper can be summarized as follows:

- We propose the ML-ECQP method, where each acoustic communication link in the UACNs adopts the LR algorithm to enable the transmitter to predict the quality of the communication channel, which is measured based on the bit error rate (BER). The LR based prediction is based on the perception of environmental characteristics and the communication system setups. Based on the predicted communication channel quality, the transmitter is able to optimally schedule when to transmit acoustic data, thus reducing the energy consumption caused by retransmissions.
- To construct the environment-aware underwater communication channel quality prediction model, we implement the underwater acoustic transmission experiments in the Furong Lake at Xiamen University to collect the field test data sets, which are used to train and validate the LR based prediction model.
- We conduct extensive simulations to demonstrate the performance of the proposed ML-ECQP method.

The rest of this paper is arranged as follows. In Section 2, we simply introduce the LR algorithm. The proposed ML-ECQP method is described in Section 3. In Section 4, we describe the underwater acoustic transmission experiments. The prediction performance of the LR based model and the energy consumption of the network by applying the ML-ECQP method are analyzed in Section 5. Finally, Section 6 concludes the paper.

2. Description of LR algorithm in machine learning

This section will introduce the principle of the LR algorithm.

2.1. Linear regression and its drawbacks

The linear regression algorithm refers to as fitting the distribution of sample points in a multidimensional space according to the linear combination of eigenvalues. Assume a data set is (X, Y) , where $X = [x_1, x_2, \dots, x_n]$ and $Y = [y_1, y_2, \dots, y_n]$ represent the eigenvectors and the labels of the samples, respectively. Then, we have the linear regression model $H(X)$ as follows:

$$H(X) = W^T X = w_0 x_0 + \sum_{i=1}^n w_i x_i, \quad (1)$$

where $x_0 = 1$ is the offset item, $W = [w_0, w_1, w_2, \dots, w_n]$ is the weight vector (where each element in the weight vector represents the weight of each eigenvector), and W^T is the transpose of the weight vector W .

Linear regression is applicable to not only regression problems, but also classification problems. In a classification problem, the linear regression algorithm divides the output value of the model into two categories based on a predefined threshold. As shown in Fig. 1 (a), several sample points are marked as red circles and green crosses in a two-dimensional space. The solid yellow line in Fig. 1 is the fitting curve, denoted as $f(x)$, derived by the linear regression model based on these data samples (i.e., red circles

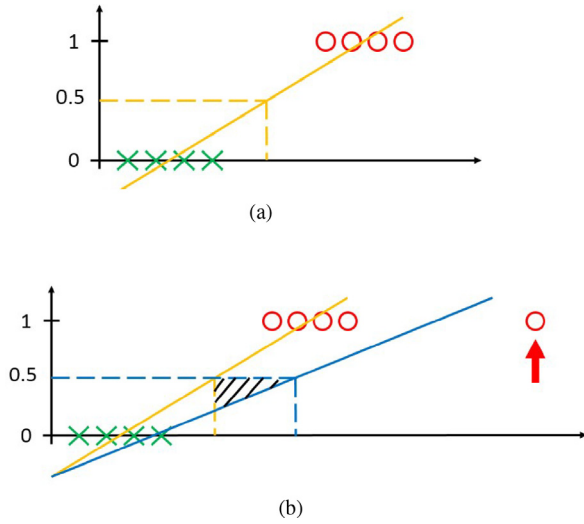


Fig. 1. The schematic diagram of the linear regression classification and its drawbacks.

and green crosses). If the threshold is set to be 0.5, then the data samples can be easily classified into two categories. That is, for any data sample (a, b), if $f(a) > 0.5$, it is in category-1 (i.e., red circle); otherwise, it is in category-0 (i.e., green cross).

However, the linear regression based classification method has many drawbacks, such as sensitive to imbalanced data and unable to classify the data samples if the output is non-continuous value [28]. For example, as shown in Fig. 1(b), if there is an abnormal data sample (i.e., a red circle indicated by an upward arrow), then the solid blue line would be the new fitting line for the updated data samples. The new fitting line would result in the data sample in the shaded area being misclassified into category-0 (i.e., green cross).

2.2. Logistic regression

The LR algorithm is proposed to resolve the mentioned drawbacks of the linear regression algorithm. In LR, the Sigmoid function is used to map any input values to the values between 0 and 1. The expression of the Sigmoid function is

$$g(z) = \frac{1}{1 + e^{-z}}, \quad (2)$$

where z is the linear regression model, which can be expressed by Eq. (1). Then, we can easily derive the LR model, denoted as $h(x)$, as:

$$y = h(x) = g[H(X)] = g(W^T X) = \frac{1}{1 + e^{-W^T X}}. \quad (3)$$

Deriving the weight of eigenvectors for the data sets, i.e., $W = [w_0, w_1, w_2, \dots, w_n]$, is the target of the LR algorithm. If a loss function $J(w)$ is defined as the difference between the base truth and the predicted values, then the training process can be transformed into a minimization problem of loss function $J(w)$ over the training set, i.e.,

$$w^* := \arg \min_w J(w). \quad (4)$$

With respect to the LR algorithm, we adopt cross entropy to describe the loss function $J(w)$. Specifically, according to Eq. (3), we can first obtain the likelihood function $L(w)$ of m data samples as follows,

$$L(w) = \prod_{i=1}^m [h(x_i)]^{y_i} [1 - h(x_i)]^{1-y_i}. \quad (5)$$

Then, Eq. (4) is transformed into the logarithmic form, i.e.,

$$l(w) = \log L(w) = \sum_{i=1}^m [y_i \log h(x_i) + (1 - y_i) \log [1 - h(x_i)]]. \quad (6)$$

Then, we can obtain the loss function $J(w)$,

$$J(w) = -\frac{1}{m} l(w). \quad (7)$$

Afterwards, the partial derivative of the loss function with respect to w is

$$\begin{aligned} \frac{\partial J(w)}{\partial w} &= -\frac{1}{m} \sum_{i=1}^m \left[y_i \frac{1}{h(x_i)} \frac{\partial h(x_i)}{\partial w_j} - (1 - y_i) \frac{1}{1-h(x_i)} \frac{\partial h(x_i)}{\partial w_j} \right] \\ &= -\frac{1}{m} \sum_{i=1}^m \left[y_i \frac{1}{g(w^T x_i)} - (1 - y_i) \frac{1}{1-g(w^T x_i)} \right] \frac{\partial g(w^T x_i)}{\partial w_j} \\ &= -\frac{1}{m} \sum_{i=1}^m [y_i (1 - g(w^T x_i)) - (1 - y_i) g(w^T x_i)] x_i^j \\ &= -\frac{1}{m} \sum_{i=1}^m [y_i - g(w^T x_i)] x_i^j \\ &= -\frac{1}{m} \sum_{i=1}^m [g(w^T x_i) - y_i] x_i^j. \end{aligned} \quad (8)$$

According to Eq. (8), the iterative update expression of w can be obtained as follows.

$$w_j := w_j - \eta \frac{1}{m} \sum_{i=1}^m [g(w^T x_i) - y_i] x_i^j, \quad (9)$$

where η represents the learning rate, i.e. the step size of each update.

Based on Eq. (9), the weights of all the eigenvectors in the LR model can be obtained by training the labeled sample points. The LR model $h(x)$ in Eq. (3) can then be derived, and $h(x)$ can be used to classify the new data sets. In addition, the problem of over-fitting may occur in the process of model training. That is, the model's fitting level to the training data set is too high, which makes the model loss a good generalization ability and unable to accurately classify/predict the results for the new data sets. In order to improve the generalization ability of the LR model, the regular term is added in the loss function, and so Eq. (7) can be rewritten into

$$J(w) = -\frac{1}{m} l(w) + \lambda \|w_p\|, \quad (10)$$

where λ is the regularization coefficient, and p is usually set to 1 or 2, which represents the L_1 and L_2 regularization, respectively. The subsequent procedures to derive iterative update expression of w based on the new loss function (i.e., Eq. (10) is very similar to Eqs. (8) and (9) (where the regular term will be added), and we do not specify the detailed derivation.

3. Description of the proposed method

Based on the mentioned LR model, we propose the ML-ECQP method, where the quality of the underwater channel is predicted. In order to derive the LR based prediction model, the experimental data of underwater acoustic transmission need to be first collected as the training sample data set to derive the weight vector W . The

feature vector of each input data sample is consisted of the environmental parameters of an underwater acoustic channel and the setups of the transmission system. The BER of an underwater acoustic channel is used as the output of the data samples. After collecting enough training samples, the LR algorithm is used to construct a model to predict the quality of an underwater acoustic channel, which is measured by the BER. Finally, through the constructed LR model, the quality of an underwater acoustic channel is predicted in advanced according to the perceived environmental parameters of the underwater acoustic channels and the setups of the transmission system. Based on the predict channel quality, the transmitter will optimize the data transmission time, i.e., preventing from transmission data when communication quality in terms of BER is bad, and thus reduce the number of retransmissions caused by transmission failures. Accordingly, the energy consumption of each sensor node in UACNs can be significantly decreased. Fig. 2 illustrates the flowchart of the proposed ML-ECQP method.

In order to ensure the performance of the above ML-ECQP method, it is necessary to guarantee the accuracy of the LR based prediction model. In the following, we will examine the performance of the proposed ML-ECQP method and the LR based link quality prediction model via extensive experiments and simulations.

4. The lake experiment of the underwater acoustic transmission

4.1. Lake experimental process

The underwater acoustic transmission experiment is carried out in Furong Lake, Xiang'an campus of Xiamen University in Fujian Province, China. The experiment is used to obtain the data samples for training and validating the LR model in the ML-ECQP method.

Fig. 3 shows the scenario that our experiments want to emulate. Two source nodes, one destination node, and one relay node are deployed to achieve the two-source single-relay communications [29], where acoustic data are transmitted from two underwater source nodes to a destination node via a relay node. Specifically, the two source nodes broadcast packets X_1 and X_2 , respectively, in different time slots. Since the relay node is close to the two source nodes, the relay node is assumed to successfully receive the two packets and generates a new packet X_R , where $X_R = X_1 \oplus X_2$ (here, \oplus is the modulo 2 sum operation). The relay node then broadcasts packet X_R . The destination node would expect to receive all the packets (i.e., X_1 , X_2 , and X_R) and apply a decoding method (either channel decoding or channel-network joint decoding) to obtain the original X_1 and X_2 packets¹[29].

Our experiments try to emulate the scenario described in Fig. 3. As shown in Fig. 4, the experiment mainly consists of two parts, i.e. the transmitter part and the receiver part. The transmitter part comprises a laptop, a National Instruments (NI) data acquisition card, an amplifier, and three underwater acoustic transducers. The laptop is used to generate the transmitted binary data streams. The NI data acquisition card is to convert digital signals into analog signals, and the amplifier is to amplify analog signals. The underwater acoustic transducer is used to transmit analog signals in the form of acoustic waves. Here, three underwater acoustic transducers are used to emulate the behaviors of two source nodes and one relay node in Fig. 3. That is, packets X_1 , X_2 , and X_R will be generated by the transmitter and emitted by the three different underwater acoustic transducers in three different time slots. The receiver part comprises a laptop, an NI data acquisition card, and

¹ Note that, as compared to directly sending packets from the source nodes to the destination node, applying the relay node to encode and transmit the packet to the destination node (which receives and decodes the original packets from the source nodes) incurs lower BER.

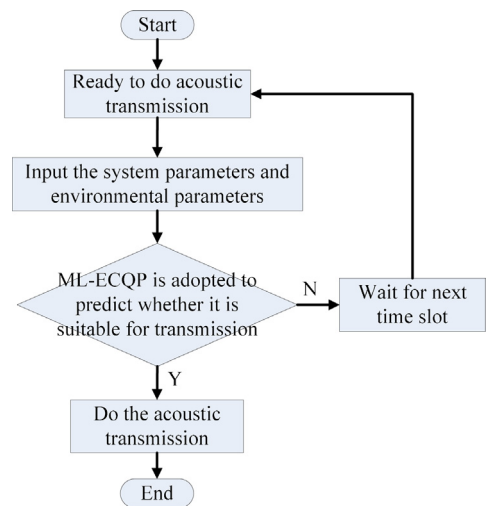


Fig. 2. Flowchart of ML-ECQP.

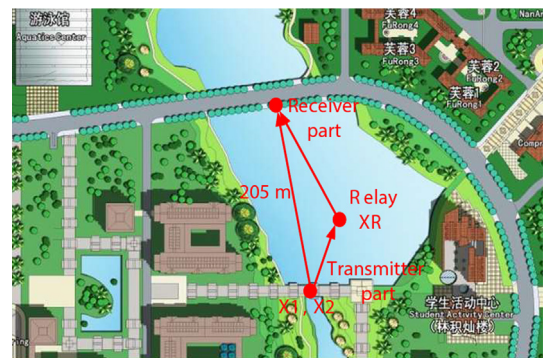


Fig. 3. The schematic diagram of the lake experimental site.

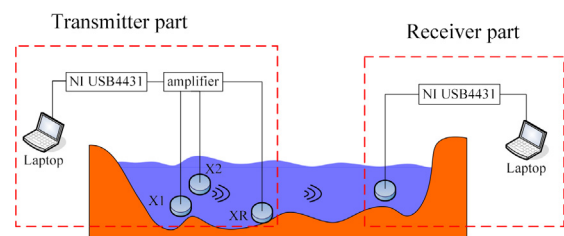


Fig. 4. The layout of the underwater acoustic communication experiment.

an underwater acoustic transducer. The underwater acoustic transducer is used to receive the acoustic waves and demodulate the acoustic waves to obtain the analog signals. The NI data acquisition card is to convert analog signals into digital signals, and the laptop is used to receive and display the digital signals. The distance between the transmitter and the receiver is around 205 meters. Note that the underwater communication channel is referred to as the channel between the transmitter and the receiver in the experiment.

The experiment setup for the underwater acoustic transmissions in the lake environment is listed in Table 1. The original bit streams are converted into analog signals based on Binary Phase Shift Keying (BPSK). Linear sweep signal is used as a synchronization head to achieve the synchronization among different nodes. In addition, two signal carrier frequencies, i.e., 23 kHz and 25 kHz, are used in the experiment to explore the relationship between the

Table 1
Parameter settings of lake experiment for the underwater acoustic transmission.

Parameter	Value
Baseband frequency	2000 Hz
Carrier frequency	23 kHz/ 25 kHz
Sample frequency	100 kHz
Code rate	1/2
Number of bits	1024
Modulation mode	BPSK
Guard interval	500 ms

carrier frequency and the quality of an underwater acoustic communication channel between the source and destination nodes. According to the parameter settings listed in Table 1, Fig. 5 shows the signal waveforms generated via MATLAB. The three signals will be transmitted by three different underwater acoustic transducers, which represent two source nodes and one relay node, respectively. There are three blocks in Fig. 5, where the first and the second blocks represent the signals for packets X_1 and X_2 sending from two underwater source nodes, respectively, and the third block represents the signal for packet X_R sending from the relay node. Here, we assume that the relay node is much closer to the destination node than the two source node (as indicated by Fig. 3), and thus the amplitude of the signal for packet X_R is set up to be higher than that for packet X_1 and X_2 . Note that, in the experiment, we can control the signal amplitude by adjusting the transmission coefficient (ranging from 0.1 to 1.0) via the program interface of the amplifier. Thus, the generated signals are transmitted repeatedly and grouped based on the values of transmission coefficient, carrier frequency, and different ways of decoding. In addition, in order to consider the how the underwater environment affects the channel condition, we also use the anemometer device to measure the hydrological parameters (such as the wind speed, the water surface temperature, and the air humidity) during each data transmission. Therefore, all the mentioned parameters in the experiment will be considered as the feature selection candidates when we construct the prediction model.

Finally, through the experiment, we obtain totally 2856 data samples, each of which is corresponding to the data for one group of underwater acoustic transmissions from the source node to the destination node via the relay node (i.e., transmitting packets X_1 , X_2 , and X_R from three different underwater acoustic transducers at the transmitter to the receiver). The involved feature variables of each collected data sample are listed in Table 2. It is worth noting that two different decoding methods, i.e., the channel decoding method (labeled as 0) and the channel-network joint decoding method (labeled as 1), are used to decode the received signals.

4.2. Preprocessing of the lake experimental data

Before using the collected experimental data samples to construct the prediction model, the integrity of the data should be guaranteed. The integrity of the data samples means that the values of each feature variables for each data sample should be non-empty and reasonable. In addition, in order to improve the generalization ability of the constructed model, it is necessary to preprocess the collected data after data sample integrity checkup.

In this paper, according to the result of BER after decoding, the collected data is classified into two categories, i.e. grade 0 and 1, where grade 0 indicates the BER of the receiver is less than 0.1 (which implies that the quality of the current communication channel is good) and grade 1 indicates the BER of the receiver is no less than 0.1 (which implies that the quality of the current communication channel is bad). That is,

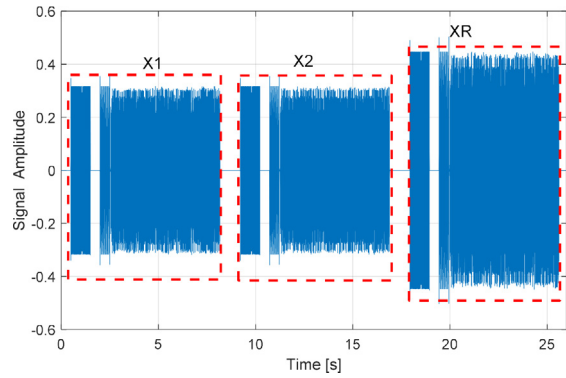


Fig. 5. The generating signal waveform using MATLAB.

Table 2
The involved feature variables of each collected data.

Feature Variable	Unit
Carrier frequency	kHz
Transmitting coefficient	\
Wind speed	m/s
Water temperature	°C
Air humidity	%
Signal to noise ratio (SNR)	dB
Decoding mode	\

$$grade = \begin{cases} 0, & BER < 0.1. \\ 1, & BER \geq 0.1. \end{cases} \quad (11)$$

The statistics of the both grades in the collected data samples are shown in Fig. 6, where 618 data samples are categorized into grade 0 and 2238 data samples are categorized into grade 1. Data samples in good communication channel quality is significantly fewer than those in bad communication channel quality, and so the collected data samples has the imbalanced distribution problem, which refers to the situation that the sample sizes of different categories are significantly imbalanced, which makes the classification algorithm concentrate on classifying the category with more data samples accurately, while ignoring the category with less data samples. To solve this problem, we should adjust the weight of each data sample to ensure that each data sample has the same impact on the prediction model. The weight adjustment rule for each sample is described as follows [30]. Assuming that the number of data samples belonging to grade 0 is N_0 , the number of data samples belonging to grade 1 is N_1 , and the weights of two grades are set to α_0 and α_1 , respectively. Thus, the weights of the two grades can be calculated by the following equation,

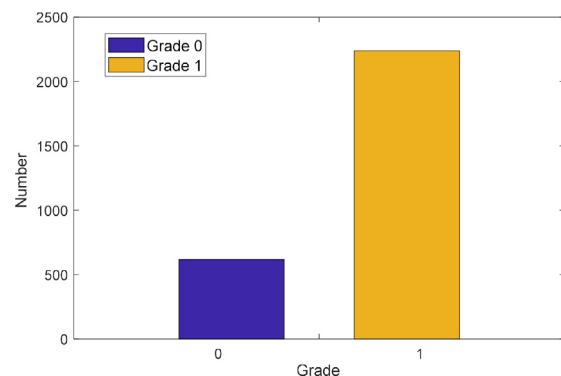


Fig. 6. The number of data samples for each grade value.

	F	AMPLITUDE	WIND	T	HUMIDITY
count	2856.000000	2856.000000	2856.000000	2856.000000	2856.000000
mean	24.000000	0.554062	0.916120	26.034174	47.359804
std	1.000175	0.284604	0.732303	5.155584	11.051325
min	23.000000	0.100000	0.000000	20.000000	29.100000
25%	23.000000	0.300000	0.400000	21.200000	36.000000
50%	24.000000	0.600000	0.800000	24.200000	49.000000
75%	25.000000	0.800000	1.250000	31.500000	58.200000
max	25.000000	1.000000	4.250000	36.500000	64.500000

	SNR	MODEL
count	2856.000000	2856.000000
mean	28.596169	0.500000
std	8.874122	0.500088
min	-9.147165	0.000000
25%	23.809210	0.000000
50%	29.614387	0.500000
75%	34.789019	1.000000
max	48.968151	1.000000

Fig. 7. The statistics of each feature variable.

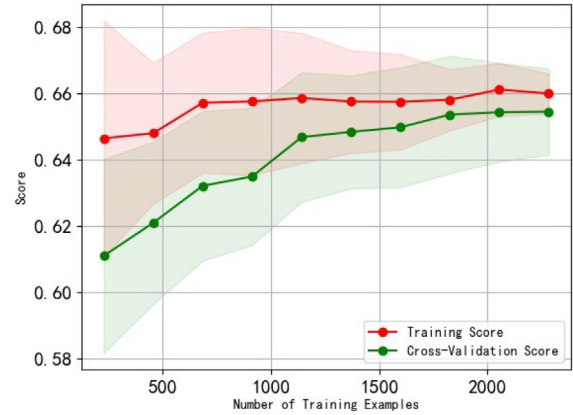


Fig. 8. The learning curve of the LR based prediction model.

$$N_0\alpha_0 = N_1\alpha_1. \quad (12)$$

Substitute Eq. (12) into Eq. (6), we have the updated likelihood function

$$l(w) = \log L(w) = \sum_{i=1}^m \alpha_j [y_i \log h(x_i) + (1 - y_i) \log [1 - h(x_i)]]. \quad (13)$$

Fig. 7 shows the statistics of each feature variable in the data samples. We can find that the statistic values of different feature variables are quite different, which will lead to the algorithm put a higher weight to the feature variable with larger values in the training process, and thus make the classification algorithm unable to be converged. Therefore, it is necessary to normalize all feature variables in order to keep them having the same impact on the prediction model and accelerate the convergence speed. We use the following formula to do the normalization.

$$x' = \frac{x - \mu}{\sigma}, \quad (14)$$

where x and x' are the data samples with respect to a feature variable before and after normalization, respectively, and μ and σ are the mean and standard deviation of a feature variable among all the data samples, respectively.

5. Prediction model construction and performance analysis

There are seven feature variables involved in the experiment, including carrier frequency, transmission coefficient, wind speed, water temperature, air humidity, SNR, and decoding mode. The number of the feature variables is far fewer than the number of data samples, and so all the feature variables can be used to construct the prediction model without having feature selection, thus reducing the complexity of the LR based prediction algorithm. When constructing the prediction model based on the LR algorithm in the proposed ML-ECQP method, we need to divide the data samples into the training data samples and the testing data samples. The training data samples are used to train the LR based prediction model to minimize the loss function, while the testing data samples are used to test the accuracy of the constructed prediction model. In order to determine the proportion of the splitting, it is necessary to draw the learning curve of the LR based prediction model, which comprises the performance curve of the training samples and the performance curve of the test samples. The learning curve, as shown in Fig. 8, reflects how the performance of the constructed model changes with respect to the increase of the number of training samples. From Fig. 8 we can derive that as the number of the training samples increases, the two learning curves gradually converges. When the proportion of the training samples reaches 80% (i.e., $2284/2856 \approx 80\%$), the performance of the model has been stabilized. Therefore, 80% of the total data

samples are used as the training samples, i.e. $N_{training} = 2856 \times 80\% \approx 2284$, and the rest of them are used as the test samples, i.e. $N_{test} = 2856 \times 20\% \approx 572$.

5.1. Performance analysis of the linear regression based prediction model

By applying the training data samples to solve Eq. (4), the weights of all the feature variables can be derived and are listed in Table 3. The positive and negative sign of a feature weight represents the positive or negative correlation between each feature and the quality of the communication channel, respectively. For example, carrier frequency and the quality of the communication channel exhibit the negative correlation, and the transmission coefficient and the quality of the communication channel shows the positive correlation. The absolute value of each feature weight indicates the correlation level between each feature and the predicted quality of the communication channel. For example, the correlation between transmission coefficient and the quality of the communication channel is much stronger than that between decoding mode and the quality of the communication channel. In order to further analyze the prediction performance of the constructed model, the confusion matrix is applied to visualize the prediction performance of the model [28]. The confusion matrix for a binary classification problem can be described as a 2×2 matrix/table, where each element in the matrix represents the number of the following four outcomes.

- True Positive (TP): the real label of the sample is positive class, and the predicted result of the model is also a positive class.
- False Negative (FN): the real label of the sample is positive class, but the predicted result of the model is a negative class.
- False Positive (FP): the real label of the sample is negative class, but the predicted result of the model is a positive class.
- True Negative (TN): the real label of the sample is negative class, and the predicted result of the model is also a negative class.

Based on the elements in the confusion matrix, the following metrics are defined to evaluate the performance of the LR based prediction model.

- 1) **Accuracy:** it represents the proportion of all correctly predicted results to the total number of training data samples, i.e.,

$$Accuracy = \frac{TP + TN}{TP + TN + FP + FN}. \quad (15)$$

Table 3
The weights of all the feature variables.

Feature variable	Weight value
Carrier frequency	-0.016180
Transmitting coefficient	0.47608302
Wind speed	0.14284686
Water temperature	-1.47350085
Air humidity	-1.63384352
Signal to noise ratio (SNR)	-0.66985144
Decoding mode	0.09308579

2) **Precision**: it represents the proportion of the correctly predicted positive results to the total number of predicted positive samples, i.e.,

$$Precision = \frac{TP}{TP + FP} \quad (16)$$

3) **Sensitivity/Recall**: it represents the proportion of the correctly predicted positive results to the total number of real positive samples, i.e.,

$$Sensitivity/Recall = \frac{TP}{TP + FN} \quad (17)$$

4) **Specificity**: it represents the proportion of the correctly predicted negative results to the total number of real negative samples, i.e.,

$$Specificity = \frac{TN}{TN + FP} \quad (18)$$

The value of each of the above metrics is between 0 and 1. Note that a larger value of any of these metrics may indicate that the LR based prediction model has a better performance. However, since the Precision and Recall values could be opposite (e.g., a prediction model could have a high Precision but a low Recall), the F_1 score is introduced to better explain the performance of the prediction model, i.e.,

$$F_1 = 2 \cdot \frac{Precision \cdot Recall}{Precision + Recall} \quad (19)$$

where the value of the F_1 score is also between 0 and 1, and a larger value of F_1 indicates a better performance for the model.

The prediction performance of the constructed LR based prediction model will be analyzed by calculating the above metrics. The confusion matrix of the constructed LR based prediction model is shown in Fig. 9, where X- and Y- axes represent the predicted and real grade values (i.e., grade 0 or grade 1) of the quality of the underwater acoustic link, respectively, and the numbers in the figure implies numbers of data samples under different predicted and real channel quality scenarios. Based on Fig. 9, we can derive the values of the five metrics for, i.e., Accuracy, Precision, Sensitivity, Specificity, and F_1 score, shown in Tables 4 and 5, where Table 4 lists the results with the grade 0 data samples (i.e. the data samples are generated when the link suffer from low BER) as the positive class, and Table 5 lists the results with the grade 1 data samples (i.e. the data samples are generated when the link suffer from high BER) as the positive class. We can observe, from Table 4, that the constructed LR based prediction model has a relatively poor prediction result i.e., a low F_1 score. Therefore, the model incurs a lower prediction accuracy when the wireless channel is in the good communication quality, and thus the transmitter may miss some appropriate transmission opportunities. From Table 5, we can find that the constructed LR based prediction model has a high F_1 score, which indicates that the model can guarantee the prediction accuracy when the channel is in the bad communication quality. As a result, the transmitter can effectively

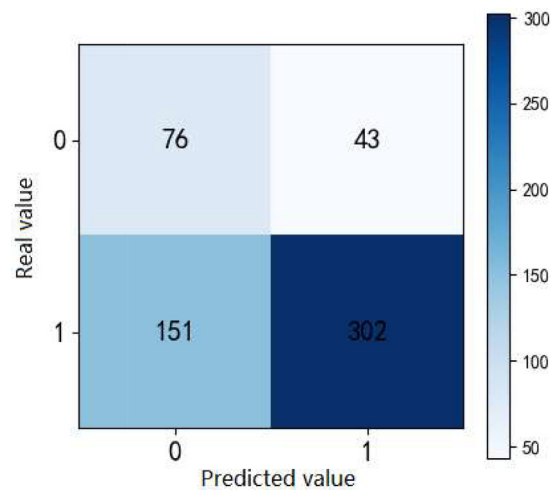


Fig. 9. The confusion matrix of the constructed LR based prediction model.

Table 4
The related indicators of the confusion matrix when grade 0 samples are the positive class samples.

Indicator	Value
TP	76
FN	43
FP	151
TN	302
Accuracy	0.66
Precision	0.33
Sensitivity (or recall)	0.64
Specificity	0.67
F_1 score	0.44

Table 5
The related indicators of the confusion matrix when the grade 1 samples are the positive samples.

Indicator	Value
TP	302
FN	151
FP	43
TN	76
Accuracy	0.66
Precision	0.88
Sensitivity (or recall)	0.67
Specificity	0.64
F_1 score	0.76

avoid the transmission in bad channel condition to reduce the number of retransmission and save more energy.

Fig. 10 shows the receiver operating characteristic (ROC) curve (denoted by yellow line) for the constructed LR based prediction model, where the X-axis represents the FP rate, and the Y-axis represents the TP rate. The blue dotted line in Fig. 10 represents the ROC curve of the random prediction model, where the probability of predicting the channel quality to be good (i.e., grade = 0) and bad (i.e., grade = 1) are the same, i.e., 0.5. Given a FP rate, a higher TP rate indicates a model can predict the channel quality more accurate. Therefore, we can observe that the LR based prediction model always incurs a higher TP rate than the random prediction model under different FP rates. Hence, the prediction accuracy of the proposed LR based prediction model is better than that of the random prediction model. However, there is still a large space for improving the performance of the LR based prediction model as

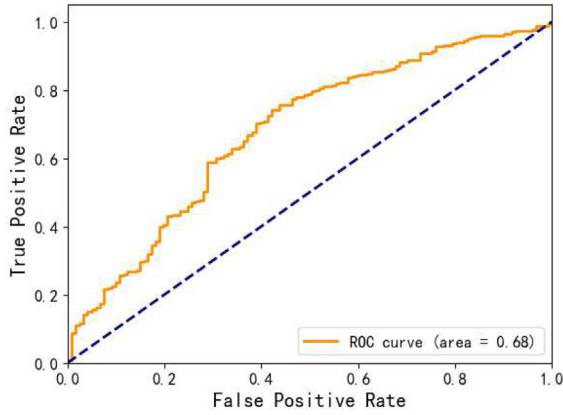


Fig. 10. The ROC curve the constructed LR based prediction model. The blue dotted line represents the prediction performance of the random prediction model.

compared to the ideal case, where the TP rate is always equal to 1 under different FP rates.

Based on above analysis, owing to the limited number of training data samples, the LR based prediction model may incur some prediction errors when the channel quality is good, but can accurately predict the bad channel quality to enable the transmitter to reduce the invalid transmissions or retransmissions, thus potentially saving the energy of the transmitter.

5.2. Performance analysis of ML-ECQP

In this section, we will analyze the performance in terms of energy consumption of the transmitters, transmission delay, and packet loss rate of the ML-ECQP algorithm, which utilizes the prediction results from the proposed LR based model to schedule the data transmission, i.e., if the predicted channel condition is good, the transmitter would transmit a packet; otherwise, the transmitter halt the transmission and wait until the channel condition becomes good. The following two methods are used as the reference algorithms to compare the performance with ML-ECQP.

1) Non-prediction algorithm: the transmitter does not predict the channel condition and transmits a packet to the receiver during each time slot.

2) Ideal-prediction algorithm: the transmitter knows the channel condition in advance. That is, the channel condition can be accurately predicted by the transmitter, which will transmit a packet when packet is good.

In the simulation, $N_{test} = 2856 \times 20\% \approx 572$ data samples are used to emulate the channel conditions. That is, each data sample represents the actual channel condition and underwater acoustic environment for a specific time slot. Assume that one packet can be transmitted from the transmitter to the receiver during each time slot. A packet can be successfully transmitted to the receiver when the current underwater channel is in good condition (i.e., $grade = 0$); otherwise, the packet needs to be retransmitted (i.e., $grade = 1$) later. Thus, if there are N_p packets needed to be transmitted, then the total energy consumption of the transmitter, denoted as E_t , is

$$E_t = \sum_{i=1}^{N_p} (1 + K_i) \cdot b \cdot \varepsilon, \quad (20)$$

where b is the number of bits in each packet, ε is the energy consumption of transmitting a bit to the receiver, and K_i is the number of retransmissions required for transmitting packet i . Here, $0 \leq K_i \leq K_{max}$, where K_{max} is the maximum number of the allowed

retransmissions. If a packet is unable to be successfully delivered the destination after K_{max} retransmissions, the packet will be dropped directly. Thus, we define the packet loss rate, denoted as η , as follows.

$$\eta = \frac{N_{loss}}{N_p}, \quad (21)$$

where N_{loss} is the number of the packets, which is unable to be delivered after K_{max} retransmissions.

Note that K_i in Eq. (20) may vary among different algorithms. For instance, in the ideal-prediction algorithm, $K_i = 0$ as the algorithm can always accurately predict the channel condition, and schedule the packet transmission when the channel condition is good to completely avoid the retransmission. In the ML-ECQP algorithm, the average value of K_i is determined by the False Negative rate (grade 1 as the positive class), i.e., the number of the wrong predictions (where the predicted channel condition is good, but the actual value is bad) over total number of the predictions. That is,

$$\bar{K}_i = \frac{TP + TN + FP + FN}{FN}, \quad (22)$$

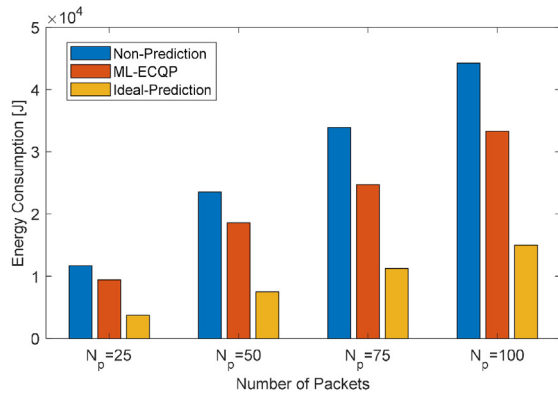
where \bar{K}_i is the average value of K_i . In the non-prediction algorithm, the value of K_i highly depends on the number of the time slots with bad channel condition.

- Performance analysis by varying the number of N_p

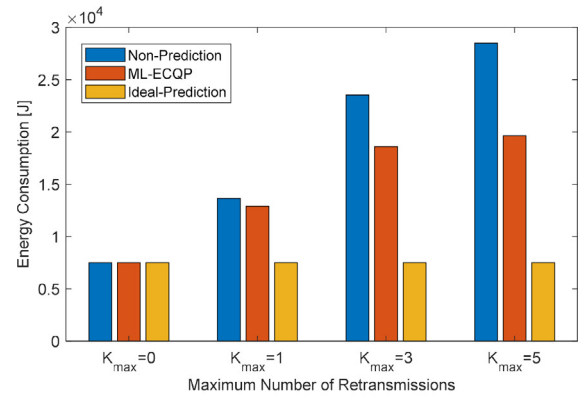
Assume that the maximum number of the allowed retransmissions $K_{max} = 3$, the number of bits in each packet $b = 1024$ bits, and the energy consumption of transmitting a bit $\varepsilon = 0.146$ J/bit. Fig. 11 shows the energy consumption E_t , the packet loss rate, and the total amount of delay for transmitting N_p packets incurred by the three algorithms under different number of packets need to be transmitted. From Fig. 11(a), we can find that ML-ECQP consumes less energy consumption than non-prediction but more energy consumption than ideal-prediction, and has the value of increases, the difference of energy consumption incurred by the three algorithms increases. The results demonstrate that transmitting packets only when the channel prediction is good can significantly save the energy of the transmitter especially when the traffic load of the transmitter is heavy. In addition, increasing the accuracy of the channel prediction model can significantly reduce the energy consumption of the transmitter for underwater communications. Similarly, in Fig. 11(b), ML-ECQP has lower η (which is calculated based on Eq. (21)) than non-prediction but higher than ideal-prediction (where $\eta = 0$), which also derives the similar conclusion, i.e., transmitting packets only when the channel prediction is good can significantly reduce the packet loss rate, and increasing the accuracy of the channel prediction model can significantly reduce η . Although transmitting packets only when the channel prediction is good can potentially reduce the energy consumption and packet loss rate, it increases the total delay for transmitting N_p packets as shown in Fig. 11(c), where ML-ECQP has higher delay than ideal-prediction because the LR based prediction model in ML-ECQP may result in False Positive prediction (grade 1 as the positive class), i.e., the real channel condition is good but predicted to be bad, thus missing the time slot for successful transmission and increasing the overall delay.

- Performance analysis by varying the number of K_{max}

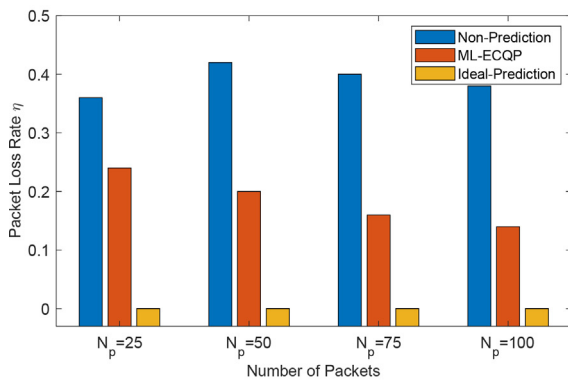
Assume that $N_p = 50$. Fig. 12 shows the performance of the three algorithms by varying K_{max} . The performance in terms of energy consumption and packet loss rate for ML-ECQP is better than non-prediction but worse than ideal-prediction as shown



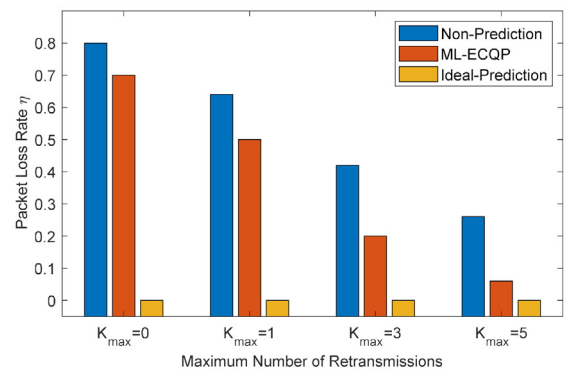
(a)



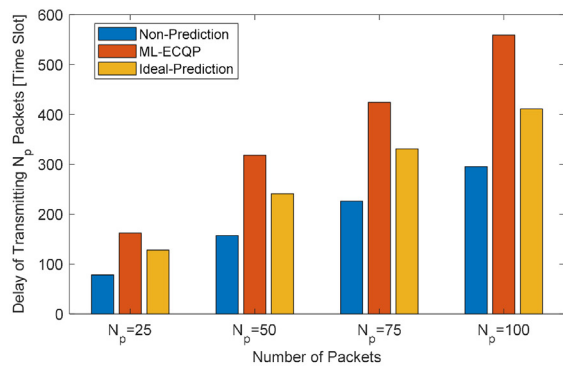
(a)



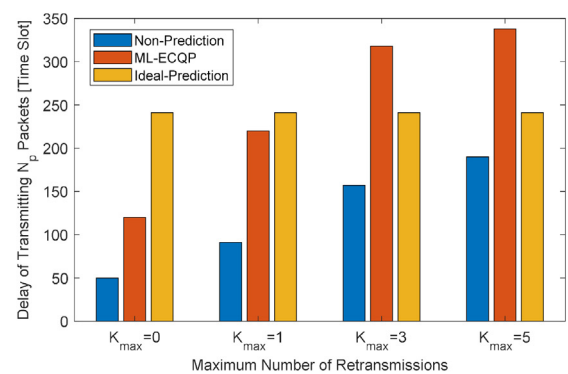
(b)



(b)



(c)



(c)

Fig. 11. The performance of the algorithms by varying the number of packets needed to be transmitted N_p .

Fig. 12. The performance of the algorithms by varying the maximum number of allowed retransmissions K_{max} .

in Fig. 12(a) and (b). Note that as K_{max} increases, the energy consumption for ML-ECQP and non-prediction increases since a larger K_{max} indicates more retransmissions triggered by the packets transmission in bad channel condition, and the energy consumption and packet loss rate for ideal-prediction does not change as K_{max} increases because ideal-prediction does not trigger any retransmissions during the whole process. Fig. 12(c) shows the overall delay of transmitting N_p packets for the three algorithms. It is interesting to see that ML-ECQP incurs a lower delay than ideal-prediction when K_{max} equals to 0 and 1. This is because the LR based prediction model in ML-ECQP may lead to False Negative predictions (grade 1 as

the positive class), i.e., the real channel condition is bad but predicted to be good, and thus ML-ECQP could schedule to transmit a packet even if the real channel condition is bad, which reduce the time of waiting for the channel to be good. For example, assume that $K_{max} = 1$ and the real channel condition in time slot t_1 and t_2 are both bad but are incorrectly predicted as both good by the LR based prediction model in ML-ECQP. Then, the delay of transmitting a packet for ML-ECQP is 2 time slots (as the packet is dropped in time slot t_2). On the other hand, ideal-prediction would wait for the real channel conduction to be good, and then transmit the packet. Thus, the delay of transmitting a packet for ideal-prediction should be longer than 2 time slots.

6. Conclusion

In this paper, we proposed an ML-ECQP method, where the LR based prediction model is used to estimate underwater channel condition between a transmitter and a receiver. Based on the estimated results, the transmitter only transmits packets when the estimated channel condition is good to reduce the number of retransmissions, thus reducing the energy consumption of the transmitter. The experiments are conducted to obtain the data samples of underwater acoustic transmissions. The data samples are used to train and test the LR based prediction model. The performance of the LR based prediction model is validated by analyzing the values of the five metrics, i.e., Accuracy, Precision, Sensitivity, Specificity, and F_1 score. In addition, extensive simulations have been conducted to demonstrate the performance of ML-ECQP as compared to other two baseline methods.

CRedit authorship contribution statement

Yougan Chen: Conceptualization, Methodology, Writing - review & editing. **Weijian Yu:** Writing - original draft. **Xiang Sun:** Writing - original draft. **Lei Wan:** Software, Writing - review & editing. **Xiaomei Xu:** Supervision, Writing - review & editing.

Declaration of Competing Interest

The authors declare that they have no known competing financial interests or personal relationships that could have appeared to influence the work reported in this paper.

Acknowledgment

The authors would like to thank Mr. Zihao Hong, Mr. Jingbo Zhou, Mr. Shenqin Huang, Mr. Jianming Wu, and Dr. Xiaokang Zhang from Xiamen University for their contributions to the discussion of this research. The authors would also like to thank Ms. Jianying Zhu, Ms. Junhui Liu, Ms. Xinrui Zhang, and Mr. Shiyu Li from Xiamen University for their help in the lake experiment.

References

- [1] Sandeep DN, Kumar V. Review on clustering, coverage and connectivity in underwater wireless sensor networks: a communication techniques perspective. *IEEE Access* 2017;5:11176–99.
- [2] Zhang H, Wang S, Sun H. A low complexity clustering optimization algorithm for underwater sensor networks. In: Proc. 2016 IEEE international conference on signal processing, communication and computing (ICSPCC). p. 1–5.
- [3] Yu W, Chen Y, Tang Y, Xu X. Power allocation for underwater source nodes in uwa cooperative networks. In: Proc. 2018 IEEE international conference on signal processing, communications and computing (ICSPCC), Qingdao; 2018. p. 1–6.
- [4] Zhu M, Wu Y. Development of underwater acoustic communication technology. *Bull Chin Acad Sci* 2019;34:289–96.
- [5] Simó DH, Chang BS, Brante G, et al. Energy consumption analysis of underwater acoustic networks using fountain codes. In: Proc. OCEANS 2016 MTS/IEEE Monterey, Monterey, CA; 2016. p. 1–4.
- [6] Pramod HB, Kumar R. Multilayered energy harvesting and aggregation in underwater sensor acoustic networks for performance enhancement. In: Proc. 2016 international conference on emerging technological trends (ICETT), Kollam. p. 1–4.
- [7] de Souza F, Souza R, Brante G, Pellenz M, Rosas F, Chang B. Code rate optimization for energy efficient delay constrained underwater acoustic communications. In: Proc. IEEE/MTS OCEANS, Genoa; 2015. p. 1–4.
- [8] L'Heureux A, Grolinger K, Elyamany HF, et al. Machine learning with big data: challenges and approaches. *IEEE Access* 2017;5:7776–97.
- [9] McQuay C, Sattar F, Driessen PF. Deep learning for hydrophone big data. In: Proc. 2017 IEEE pacific rim conference on communications, computers and signal processing (PACRIM), Victoria, BC; 2017. p. 1–6.
- [10] Roberts PLD, Jaffe JS, Trivedi MM. Multiview, broadband acoustic classification of marine fish: a machine learning framework and comparative analysis. *IEEE J Ocean Eng* 2011;36:90–104.
- [11] Chen Y, Xu X. The research of underwater target recognition method based on deep learning. In: Proc. 2017 IEEE international conference on signal processing, communications and computing (ICSPCC), Xiamen; 2017. p. 1–5.
- [12] Yang H, Gan A, Chen H, et al. Underwater acoustic target recognition using svm ensemble via weighted sample and feature selection. In Proc. 2016 13th international bhurban conference on applied sciences and technology (IBCAST), Islamabad; 2016. p. 522–7.
- [13] Pinheiro BC, Moreno UF, de Sousa JTB, et al. Kernel-function-based models for acoustic localization of underwater vehicles. *IEEE J Ocean Eng* 2017;42:603–18.
- [14] Pinheiro BC, Moreno UF. Empirical model auv localization. In: Proc. 2014 symposium on automation and computation for naval, offshore and subsea (NAVCOMP), Rio Grande; 2014. p. 1–4.
- [15] Houégnyan L, Safari P, Nadeu C, et al. Machine and deep learning approaches to localization and range estimation of underwater acoustic sources. In: Proc. 2017 IEEE/OES acoustics in underwater geosciences symposium (RIO Acoustics), Rio de Janeiro; 2017. p. 1–6.
- [16] Hu T, Fei Y. Qelar: A machine-learning-based adaptive routing protocol for energy-efficient and lifetime-extended underwater sensor networks. *IEEE Trans Mobile Comput* 2010;9:796–809.
- [17] Wang P, Wang T. Adaptive routing for sensor networks using reinforcement learning. In: Proc. the sixth IEEE international conference on computer and information technology (CIT'06), Seoul; 2006. p. 1–6.
- [18] Caro GD, Dorigo M. Ant colonies for adaptive routing in packet-switched communications networks. In: Proc. fifth int'l conf. parallel problem solving from nature; 1998. p. 673–82.
- [19] Gunes M, Sorges U, Bouazizi I. Ara-the ant-colony based routing algorithm for manets. In: Proc. international conference on parallel processing workshop, Vancouver, BC, Canada; 2002. p. 79–85.
- [20] Kamali S, Opatrný J. A position based ant colony routing algorithm for mobile ad-hoc networks. *J Netw* 2008;3:31–41.
- [21] Chen Y, Zhu J, Wan L, Huang S, Zhang X, Xu X. Acofa-fusion dynamic coded cooperation routing for different scale multi-hop underwater acoustic sensor networks. *IEEE Access* 2020;8:186773–88.
- [22] Ayalew L, Yamagishi H. The application of gis-based logistic regression for landslide susceptibility mapping in the kakuda-yahiko mountains, central japan. *Geomorphology* 2005;65:15–31.
- [23] Cannarile F, Compare M, Baraldi P, et al. Elastic net multinomial logistic regression for fault diagnostics of on-board aeronautical systems. *Aerosp Sci Technol* 2019;94(105392).
- [24] Yu FW, Ho WT. Load allocation improvement for chiller system in an institutional building using logistic regression. *Energy Build* 2019;201:10–8.
- [25] Yang D, He Y, Wu B, et al. Drinking water and sanitation conditions are associated with the risk of malaria among children under five years old in sub-saharan africa: A logistic regression model analysis of national survey data. *J Adv Res* 2020;21:1–13.
- [26] Seo Y, On B, Jang B, Im S, Seo I. Underwater cylinder recognition using machine learning with dft-based feature vectors. In: Proc. 2018 international conference on electronics, information, and communication (ICEIC), Honolulu, HI, USA; 2018. p. 1–2.
- [27] Kalaivasu V, Vishnu H, Mahmood A, Chitre M. Predicting underwater acoustic network variability using machine learning techniques. In: Proc. IEEE/MTS OCEANS 2017, Anchorage, AK, USA; 2017. p. 1–7.
- [28] Wang J, Zhou Z, Zhou A. Machine learning and its applications. In: Beijing: Tsinghua Press; 2006. p. 79–85.
- [29] Jin X. Study on joint channel-network encoding and decoding for underwater acoustic cooperative networks. M.S. thesis, Xiamen University, Xiamen, China, 1; 2017. p. 1–60.
- [30] He H, Garcia EA. Learning from imbalanced data. *IEEE Trans Knowl Data Eng* 2009;21:1263–84.

Yougan Chen (Senior Member, IEEE) received the B.S. degree from the Northwestern Polytechnical University (NPU), Xi'an, China, in 2007 and the Ph.D. degree from Xiamen University (XMU), Xiamen, China, in 2012, both in communication engineering. He visited the Department of Electrical and Computer Engineering, University of Connecticut (UConn), Storrs, CT, USA, from November 2010 to November 2012. Since 2013, he has been with the College of Ocean and Earth Sciences, XMU, where he is currently an Associate Professor of Applied Marine Physics and Engineering. His research includes the application of electrical and electronics engineering to the oceanic environment, with recent focus on cooperative communication and artificial intelligence for underwater acoustic channels. He has been served as an Associate Editor of IEEE Access, since 2019.

Weijian Yu (Student Member, IEEE) received B.S., M.S. degrees in marine technology from Xiamen University (XMU), Xiamen, China, in 2017 and 2020, respectively. His research interests focus on signal processing, cooperative communications, and artificial intelligence for underwater acoustic channels.

Xiang Sun (Member, IEEE) is Assistant Professor of Electrical and Computer Engineering at the University of New Mexico. He received the B.E. and M.E. degrees from the Hebei University of Engineering in 2008 and 2011, respectively, and the Ph.D. degree in electrical engineering from the New Jersey Institute of Technology (NJIT) in 2018. His research interests include mobile edge computing, cloud computing, Internet of Things, wireless networks, big-data-driven networking, and green

communications and computing. He is currently an Associate Editor of Digital Communications and Networks.

Lei Wan (Member, IEEE) received the B.S. degree in electronic information engineering from Tianjin University (TJU), Tianjin, China, in 2006, the M.S. degree in signal and information processing from Beijing University of Posts and Telecommunications (BUPT), Beijing, China, in 2009, and the Ph.D. degree in electrical engineering from the University of Connecticut (UConn), Storrs, CT, USA, in 2014. Currently, he is an Associate Professor with the School of Informatics, Xiamen University (XMU), Xiamen, China. His research interests include the algorithm design, system development and performance analysis for underwater acoustic communication systems. Dr. Wan is the Associate Editor for the IEEE Open Journal of Communications Society.

Yi Tao (Member, IEEE) received the B.S. degree in computer science and applications from Hangzhou Dianzi University, China, in 1998, the M.S. degree in com-

putational fluid mechanics (SIAMM) from Shanghai University, China, in 2003, and the Ph.D. degree in marine sciences from Xiamen University (XMU), China, in 2008. Since 2008, he has been an Assistant Professor with the Department of Applied Marine Physics and Engineering, XMU. His research interests include marine acoustic signal processing and underwater acoustic communication.

Xiaomei Xu received the B.S., M.S., and Ph.D. degrees in marine physics from Xiamen University (XMU), Xiamen, China, in 1982, 1988, and 2002, respectively. She was a Visiting Scholar with the Department of Electrical and Computer Engineering, Oregon State University, Corvallis, OR, USA (1994–1995). She visited the Department of Electrical and Computer Engineering, University of Connecticut (UConn), Storrs, CT, USA, as a Senior Visiting Scholar in 2012. She is now a Full Professor with the Department of Applied Marine Physics and Engineering, XMU. Her research interests lie in the fields of marine acoustics, underwater acoustic telemetry and remote control, underwater acoustic communication, and signal processing.